

3. SYMMETRY ASPECTS OF PHASE TRANSITIONS, TWINNING AND DOMAIN STRUCTURES

Table 3.4.4.6. Symmetry properties of ferroelastic domain twins and compatible domain walls

$T_{ij}$	$\bar{J}_{ij}$	Classification		$K_{ij}[F_1]$
1	$\underline{2}$	V	AR	$4^*[2], \bar{4}^*[2], 6[2], 6/m[2]$
1	$\underline{2}$	V	AR	
1	$2^*$	W	AR*	$\left\{ \begin{array}{l} 2^*[1], 422[2], \bar{4}2m[m], 32[2], \bar{3}m[m], 622[2], \bar{6}m2[m], \\ 432[222], m\bar{3}m[mm2], m\bar{3}m[2_{xy}][mm2] \end{array} \right.$
$\underline{2}^*$	$\underline{2}^*$	V	SI	
1	$2^*$	W	AR*	$23[3], 432[4], 432[3], m\bar{3}m[\bar{4}]$
$\underline{2}^*$	$\underline{2}^*$	W	SI	
1	$m^*$	V	AR*	$\left\{ \begin{array}{l} m^*[1], 4mm[m], \bar{4}2m[2], 3m[m], \bar{3}m[2], 6mm[m], \bar{6}m2[2], \\ 43m[mm2], m\bar{3}m[222], m\bar{3}m[m^*_{xy}][m2m] \end{array} \right.$
$\underline{m}^*$	$\underline{m}^*$	W	SI	
1	$m^*$	W	AR*	$m\bar{3}[3], \bar{4}3m[\bar{4}], 43m[3], m\bar{3}m[4]$
$\underline{m}^*$	$\underline{m}^*$	W	SI	
$\underline{2}^*$	$2^*2^*2$	W	SR	$\left\{ \begin{array}{l} 2^*2^*2[2], 4^*22^*[222], \bar{4}^*2^*m[mm2], 622[222], 6/mmm[mm2], \\ 432[422], 432[32], m\bar{3}m[42m] \end{array} \right.$
$\underline{2}^*$	$\underline{2}^*2^*2$	W	SR	
$\underline{2}^*$	$\underline{2}^*/m^*$	V	SR	$2^*/m^*[\bar{1}], 4/mmm[2/m], \bar{3}m[2/m], 6/mmm[2/m],$ $m\bar{3}m[mmm]$
$\underline{m}^*$	$2^*/m^*$	W	SR	
$\underline{2}^*$	$\underline{2}^*/m^*$	W	SR	$m\bar{3}[\bar{3}], m\bar{3}m[4/m], m\bar{3}m[\bar{3}]$
$\underline{m}^*$	$2^*/m^*$	W	SR	
$m$	$m$	V	AI	$4/m[m], \bar{6}[m], 6/m[m]$
$m$	$m$	V	AI	
$m$	$\underline{2}/m$	V	AR	$4^*/m[2/m], 6/m[2/m]$
$m$	$\underline{2}/m$	V	AR	
$\underline{m}^*$	$m^*\underline{m}^*\underline{2}$	W	SR	$\left\{ \begin{array}{l} m^*m^*2[2], 4^*mm^*[mm2], \bar{4}^*2m^*[222], 6mm[mm2], \\ 6/mmm[222], 43m[42m], m\bar{3}m[422], m\bar{3}m[32] \end{array} \right.$
$\underline{m}^*$	$\underline{m}^*m^*\underline{2}$	W	SR	
$m$	$m^*2^*m$	W	AR*	$\left\{ \begin{array}{l} m^*2^*m[m], 4/mmm[2mm], \bar{6}m2[m2m], 6/mmm[m2m], \\ 43m[3m], m\bar{3}m[4mm], m\bar{3}m[42m], m\bar{3}m[3m] \end{array} \right.$
$\underline{m}^*\underline{2}^*m$	$\underline{m}^*\underline{2}^*m$	W	SI	
$\underline{m}^*\underline{2}^*m$	$\underline{m}^*m^*m$	W	SR	$\left\{ \begin{array}{l} m^*m^*m[2/m], 4^*/mmm^*[mmm], 6/mmm[mmm], \\ m\bar{3}m[4/mmm], m\bar{3}m[3m] \end{array} \right.$
$\underline{2}^*m^*m$	$m^*m^*m$	W	SR	

$$w = \sqrt{2\delta/\alpha(T_c - T)}. \tag{3.4.4.27}$$

This dependence, expressed in relative dimensionless variables  $\xi/w$  and  $\eta/\eta_0$ , is displayed in Fig. 3.4.4.6.

The wall profile  $\eta(\xi)$  expressed by solution (3.4.4.26) is an odd function of  $\xi$ ,

$$\eta(-\xi) = \eta_0 \tanh(-\xi/w) = -\eta_0 \tanh(\xi/w) = -\eta(\xi), \tag{3.4.4.28}$$

and fulfils thus the condition (3.4.4.24) of a symmetric wall.

The wall thickness can be estimated from electron microscopy observations, or more precisely by a diffuse X-ray scattering technique (Locherer *et al.*, 1998). The effective thickness  $2w$  [see equation (3.4.4.26)] in units of crystallographic repetition length  $A$  normal to the wall ranges from  $2w/A = 2$  to  $2w/A = 12$ , *i.e.*  $2w$  is about 10–100 nm (Salje, 2000*b*). The temperature dependence

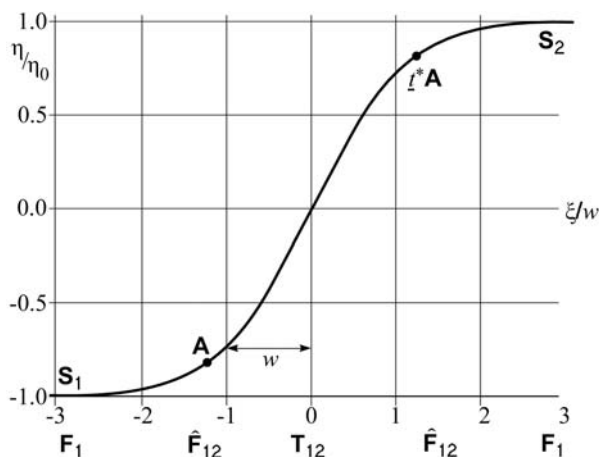


Fig. 3.4.4.6. Profile of the one-component order parameter  $\eta(\xi)$  in a symmetric wall (S). The effective thickness of the wall is  $2w$ .

of the domain wall thickness expressed by equation (3.4.4.27) has been experimentally verified, *e.g.* on  $\text{LaAlO}_3$  (Chrosch & Salje, 1999).

The energy  $\sigma$  of the domain wall per unit area equals the difference between the energy of the twin and the energy of the single-domain crystal. For a one nonzero component order parameter with the profile (3.4.4.26), the wall energy  $\sigma$  is given by (Strukov & Levanyuk, 1998)

$$\sigma = \int_{-\infty}^{\infty} [\Phi(\eta(\xi)) - \Phi(\eta_0)] d\xi = \frac{2\sqrt{2\delta}}{3\beta} [\alpha(T_c - T)]^{3/2}, \tag{3.4.4.29}$$

where  $2w$  is the effective thickness of the wall [see equation (3.4.4.27)] and the coefficients are defined in equation (3.4.4.25).

The order of magnitude of the wall energy  $\sigma$  of ferroelastic and non-ferroelastic domain walls is typically several millijoule per square metre (Salje, 2000*b*).

**Example 3.4.4.3.** In our example of a ferroelectric phase transition  $4_z/m_z m_x m_{xy} \supset 2_x m_y m_z$ , one can identify  $\eta$  with the  $P_1$  component of spontaneous polarization and  $\xi$  with the axis  $y$ . One can verify in Fig. 3.4.4.6 that the symmetry  $T_{12}[010] = \underline{2}_z^*/m_z$  of the twin ( $S_1[010]S_2$ ) with a zero-thickness domain wall is retained in the domain wall with symmetric profile (3.4.4.26): both non-trivial symmetry operations  $\underline{2}_z^*$  and  $\underline{1}_z^*$  transform the profile  $\eta(y)$  into an identical function.

This example illustrates another feature of a symmetric wall: All non-trivial symmetry operations of the wall are located at the central plane  $\xi = 0$  of the finite-thickness wall. The sectional group  $T_{12}$  of this plane thus expresses the *symmetry of the central layer* and also the *global symmetry* of a symmetric wall (twin). The *local symmetry* of the off-centre planes  $\xi \neq 0$  is equal to the face group  $\hat{F}_{12}$  of the the layer group  $T_{12}$  (in our example  $\hat{F}_{12} = \{1, m_z\}$ ).